

Supplementary information

Atypical Hydrogenation Selectivity of Platinum by Reactive Environment Modulation

Jurjen Cazemier,^{a,‡} Moussa Zaarour,^{a,‡} Sarah Komaty,^a Polina Lavrik,^a Antonio Aguilar Tapia,^b Sudheesh Kumar Veeranmaril,^a Jean-Louis Hazemann^c and Javier Ruiz-Martinez^{a,d,*}

‡These authors contributed equally to this work.

^a*King Abdullah University of Science and Technology, KAUST Catalysis Center (KCC), Catalysis Nanomaterials and Spectroscopy (CNS), Thuwal 23955, Saudi Arabia*

^b*Institut de Chimie Moléculaire de Grenoble, UAR2607 CNRS Université Grenoble Alpes, Grenoble F-38000 (France)*

^c*Institut Néel, UPR 2940 CNRS - Université Grenoble Alpes, Grenoble F-38000 (France)*

^d*Chemical Engineering Program, Physical Science and Engineering (PSE) Division, King Abdullah University of Science and Technology, Saudi Arabia.*

* *Corresponding author: javier.ruizmartinez@kaust.edu.sa*

Contents

Characterization techniques.....	3
Supplementary figures	4
XRD	4
Nitrogen physisorption.....	5
STEM images.....	5
Nanoparticle location determination in Pt@S-1-in	6
XANES	8
EXAFS	10
Activity determination and encapsulation test	11
Cinnamaldehyde hydrogenation	12
Support polarity.....	15
Shell representation	18
CO chemisorption	18
Recyclability test.....	19
Supplementary tables.....	20
Encapsulation test	21
Cinnamaldehyde hydrogenation	21
References.....	24

Characterization techniques

The platinum content within the zeolite samples was determined by inductively coupled plasma optical emission spectroscopy (ICP-OES) using Agilent 5110 ICP-OES.

Powder X-ray Diffraction Patterns were recorded using a Bruker D8 Advance instrument with Cu K α radiation ($\lambda = 0.15418$ nm) operated at 40 kV and 40 mA.

Nitrogen adsorption and desorption isotherms were measured at liquid temperature (77 K) on a Micromeritics ASAP 2020 volumetric adsorption analyzer. Prior to the adsorption analysis, all the samples were degassed under vacuum at 350 °C for 12 h. The surface area was determined by the Brunauer–Emmett–Teller (BET) method and the micropore volume was estimated by alpha-plot method using Silica-1000 (22.1 m²·g⁻¹ assumed) as a reference.

Pt L3-edge (11564 eV) XAS spectra were obtained at the European Synchrotron Radiation Facility (Grenoble, France) on the CRG-FAME beamline (BM30). The ring was operated at 6 GeV with a nominal current of 200 mA in 7/8+1 mode. The beamline is equipped with a liquid-nitrogen-cooled doubled crystal Si(220) monochromator surrounded by two Rh-coated mirrors for harmonic rejection.¹ The beam size on the sample was 210x100 μ m (HxV, FWHM). Spectra collected in transmission mode were obtained using silicon diodes under air at atmospheric pressure. The monochromator was energy calibrated measuring the Pt L3 absorption edge using a metallic platinum foil. First maximum of the 1st derivative of the absorption L3-edge is set at 11564 eV. Fluorescence spectra were collected using a CANBERRA 13-elements Ge solid state detector.

In-situ XAS characterization was performed in a high-temperature continuous-flow reactor.² The conditions were chosen to mimic the manner in which the catalyst is handled during a reaction as closely as possible including reduction, transfer to the batch reactor, and the reaction; calcined Pt@S-1-in-I (59.9 mg, 150 – 250 μ m) is added to the glassy carbon tube plugged with quartz wool (70 mg) such that the catalyst bed is completely positioned in the beam path. The catalyst was heated up to 300 °C (10 °C/min) under pure hydrogen (10 mL/min) and XANES spectra were collected until no more changes were observed, then EXAFS spectra were collected. The reactor is cooled down under a helium flow (10 mL/min) to room temperature and a flow of zero-air (10 mL/min) is introduced to the cell in order to mimic the transfer of the sample to the batch reaction under atmospheric conditions. The sample was characterized by XAS spectra under these conditions. Lastly, the reactor is heated up to 100 °C (10 °C/min) under hydrogen flow (10 mL/min) and, once no more change is observed in the XANES spectra, EXAFS spectra are collected to

investigate catalyst behavior at conditions similar to the reaction temperature. Data processing was performed using the IFEFFIT software package.³ The XANES and EXAFS spectra were obtained after performing standard procedures for pre-edge subtraction, normalization, polynomial removal, and wavevector conversion.

Supplementary figures

XRD

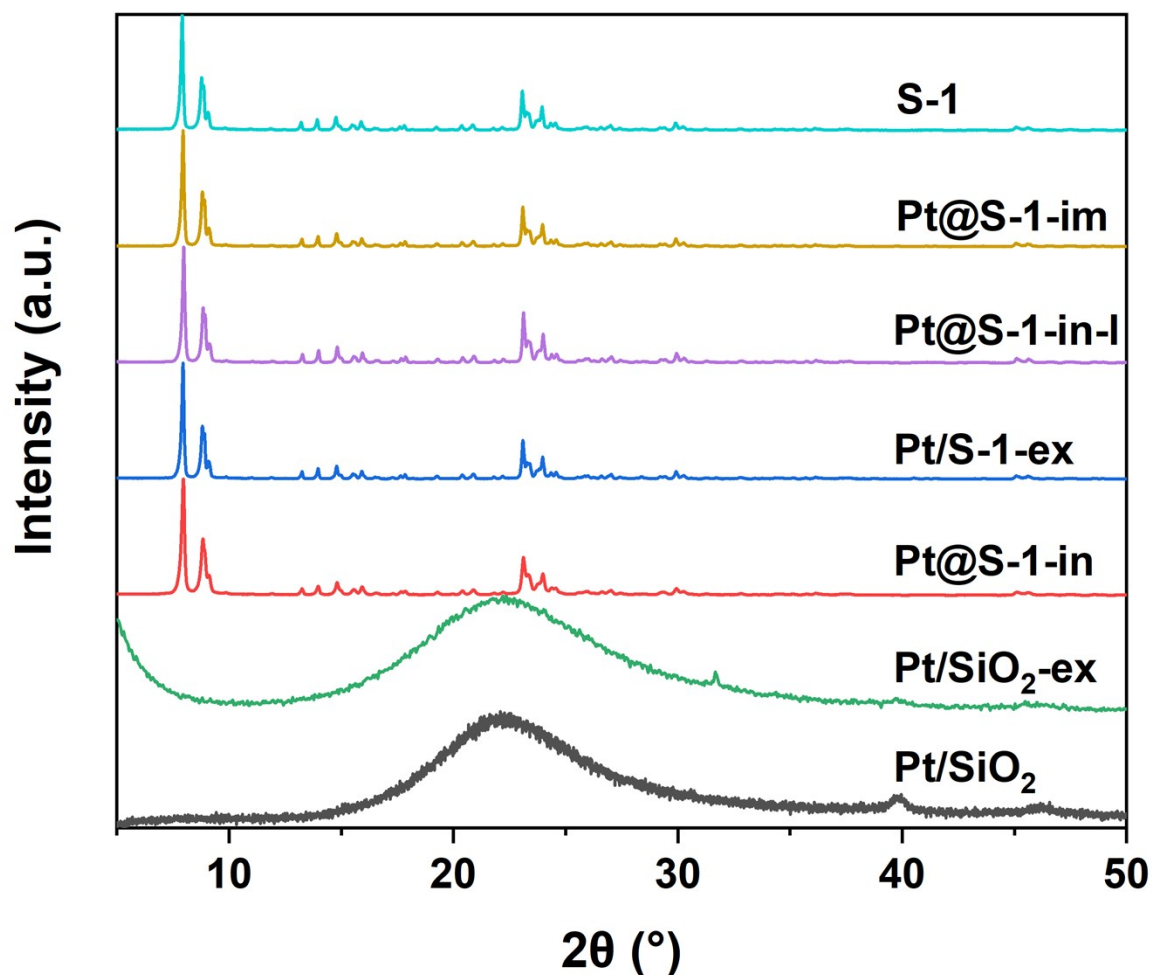


Fig. S1. Powder X-ray diffraction patterns of the various catalysts.

No reflections from Pt crystalline phases were observed in Pt@S-1-in, Pt@S-1-in-l, and Pt@S-1-im because of their small particle sizes and low loadings. Furthermore, based on the obtained XRD spectra, the presence of platinum precursor and excess ethylene diamine during the in-situ synthesis did not affect the crystallinity of the silicalite-1.

Nitrogen physisorption

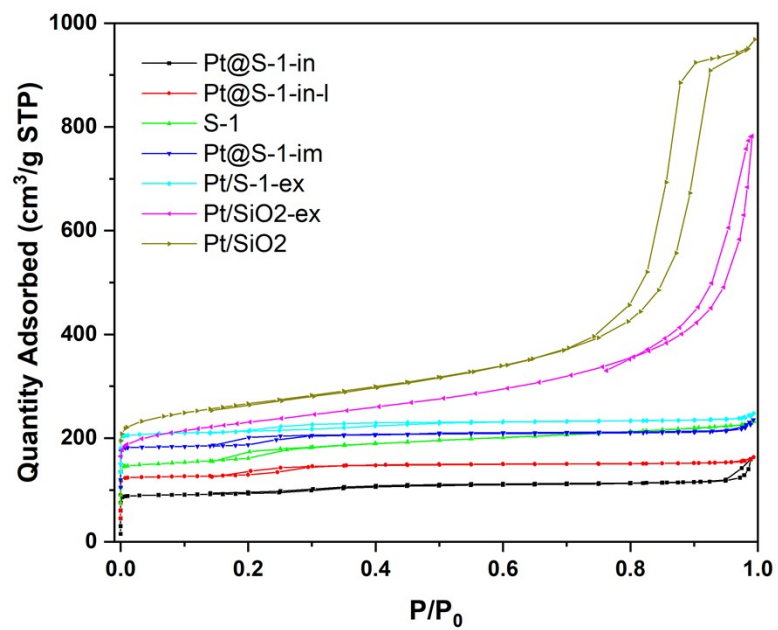


Fig. S2. Nitrogen physisorption isotherms of the various catalysts. Isotherms are offset for clarity.

STEM images

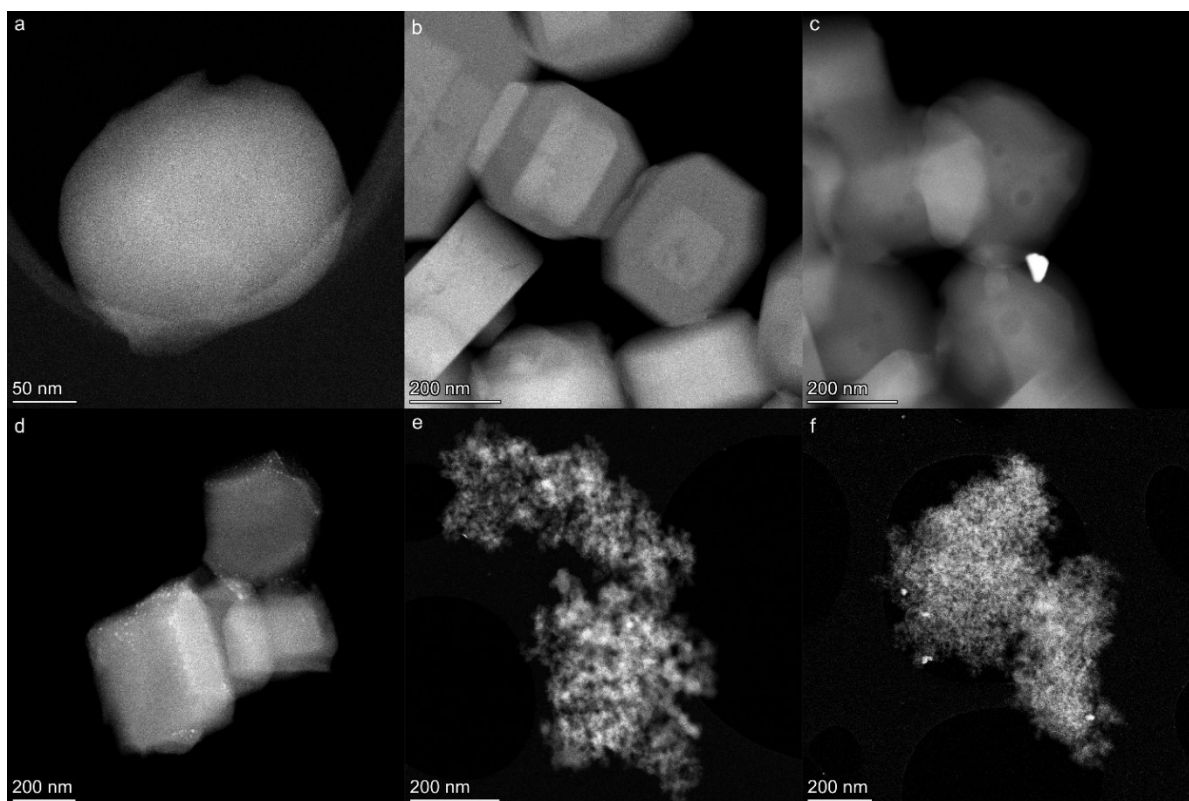


Fig. S3. HAADF-STEM images displaying the support morphologies of (a) Pt@S-1-in, (b) Pt@S-1-in-l, (c) Pt@S-1-im, (d) Pt/S-1-ex, (e) Pt/SiO₂-ex, (f) Pt/SiO₂.

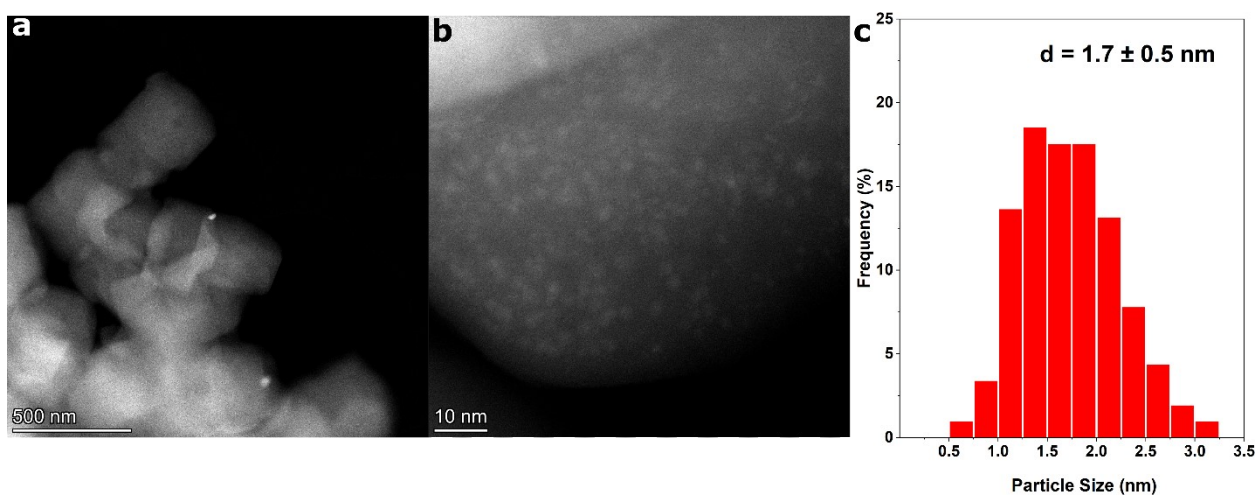


Fig. S4. (a,b) HAADF-STEM images and (c) particle size distributions of Pt@S-1-im.

Nanoparticle location determination in Pt@S-1-in

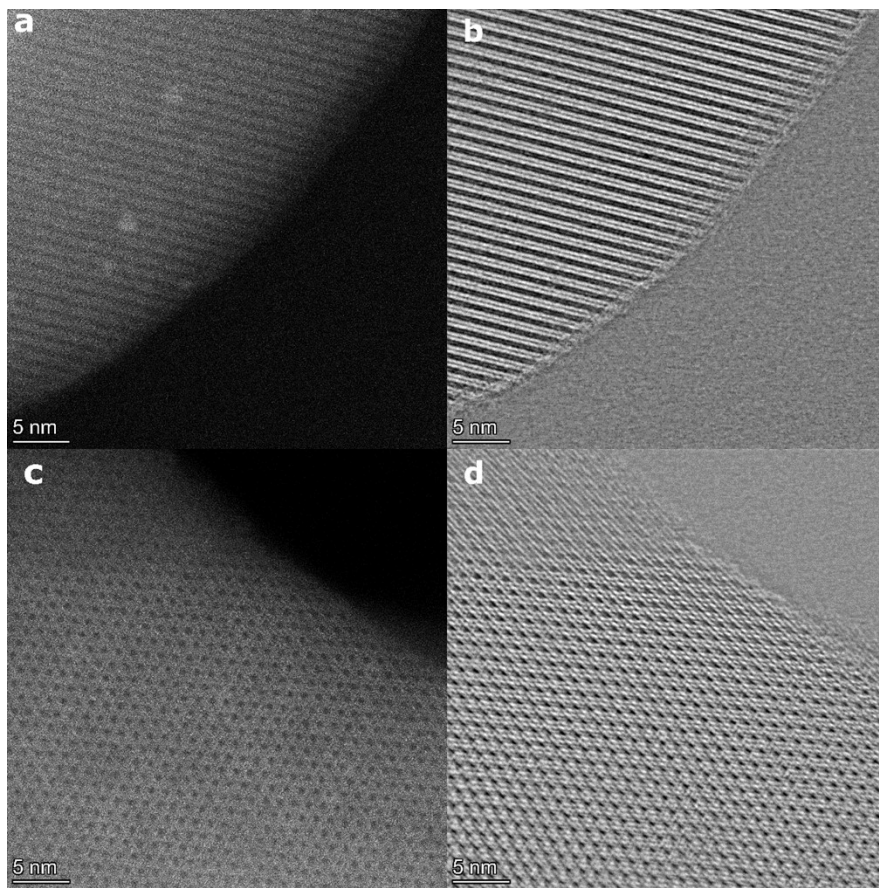


Fig. S5. (a,c) HAADF-STEM images and (b,d) accompanying iDPC-STEM images of Pt@S-1-in. The absence of Pt NPs (observed as bright spots) from the straight channels (dark holes and lines) indicates that they are located in the sinusoidal channels.

XANES

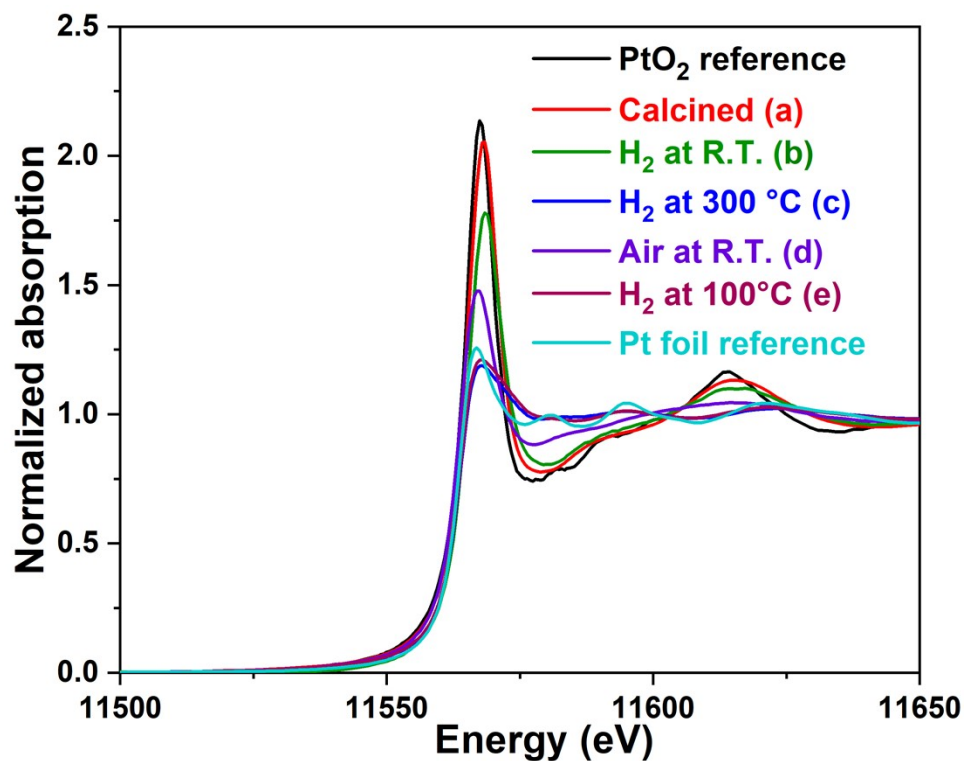


Fig. S6. Pt L3-edge XANES data of (a) calcined Pt@S-1-in-I under air followed by (b) at RT prior to reduction, (c) reduction under H₂ at 300 °C, (d) air flow at RT after reduction, and (e) H₂ flow at 100 °C.

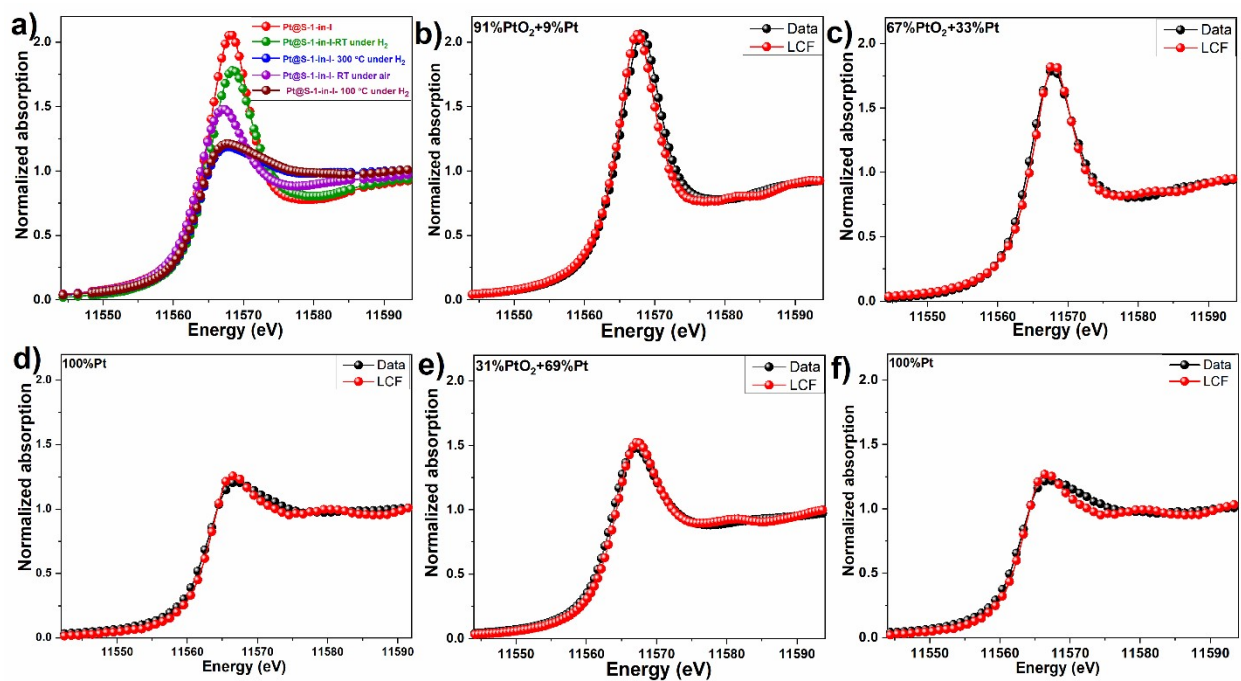


Fig. S7. (a) Pt L3-edge XANES data of Pt@S-1-in-I catalyst and the resulting LCFs of (b) calcined Pt@S-1-in-I under air at room temperature followed by (c) H₂ at RT prior to reduction, (d) reduction under H₂ at 300 °C, (e) air flow at RT after reduction, and (f) H₂ flow at 100 °C.

Information on the oxidation state of the Pt NPs in the encapsulated catalysts under various conditions was obtained by means of an *in-situ* XAS experiment (Fig. S6). For this purpose, a Pt NPs in S-1 catalyst prepared by *in-situ* encapsulation (Pt@S-1-in-I) was studied in an *in-situ* reaction cell.² The employed conditions include the reduction under H₂ at 300 °C, and approximations of the transfer to the batch reactor at room temperature during which the catalyst is briefly exposed to air, and the CAL hydrogenation conditions (100 °C under H₂). The white line intensity of the Pt L₃ edge is a signature of valence states in the Pt 5d bands and can provide information about the oxidation state.⁴

The X-ray Absorption Near Edge Structure (XANES) region is not temperature sensitive and thus allowed for linear combination fitting (LCF) of the catalyst during the whole process. Pt foil and PtO₂ reference spectra were used for the LCF approach, and the corresponding LCF-fitted results have been presented in Fig. S7.

The white line intensity of the calcined Pt@S-1-in-1 catalyst collected at room temperature (Fig. S6) is close to that of PtO₂ reference, suggesting that the Pt NPs are in the oxidized state Pt(IV), which is confirmed by LCF (Fig. S7b). Note that LCF under H₂ flow prior to reduction revealed that some degree of reduction was already apparent under such conditions, even though the majority (67 %) of the Pt remained in the oxidic phase (Fig. S7c). However, after reduction at 300 °C under H₂, the XANES spectrum closely resembles the one of Pt foil spectrum (Fig. S6), suggesting the reduction of Pt to its zerovalent state. The shoulder that can be observed originated from chemisorbed H₂.⁵ The LCF result indicates that the Pt nanoparticles are fully reduced under the reduction environment (Fig. S7d).

While this catalyst was initially expected to be stable under air, an increase in the white line intensity is observed upon exposure to air at room temperature, indicating an oxidation of Pt. However, the white line intensity did not reach the same level of intensity as observed in the calcined sample suggesting only a partial oxidation occurs under these conditions. LCF analysis substantiates this claim, as it reveals that only a fraction of Pt is oxidized (31% PtO₂) following exposure to air (Fig. S7e).

After further reduction at 100 °C under H₂, the white line intensity again resembles that of metallic Pt foil, indicating the re-reduction of Pt (Fig. S8). LCF analysis confirms the full reduction to Pt⁰ (Fig. 7f).

This result is an indication that Pt@S-1-in-I could be fully reduced under reaction conditions, however, it is important to note that the conditions utilized in this study are merely an approximation of the reaction conditions in the CAL hydrogenation process. Nonetheless, given the extended reaction times and higher hydrogen pressure associated with the CAL hydrogenation, it is unlikely that the presence of PtO₂ exerts a significant influence on the HCAL selectivity.

EXAFS

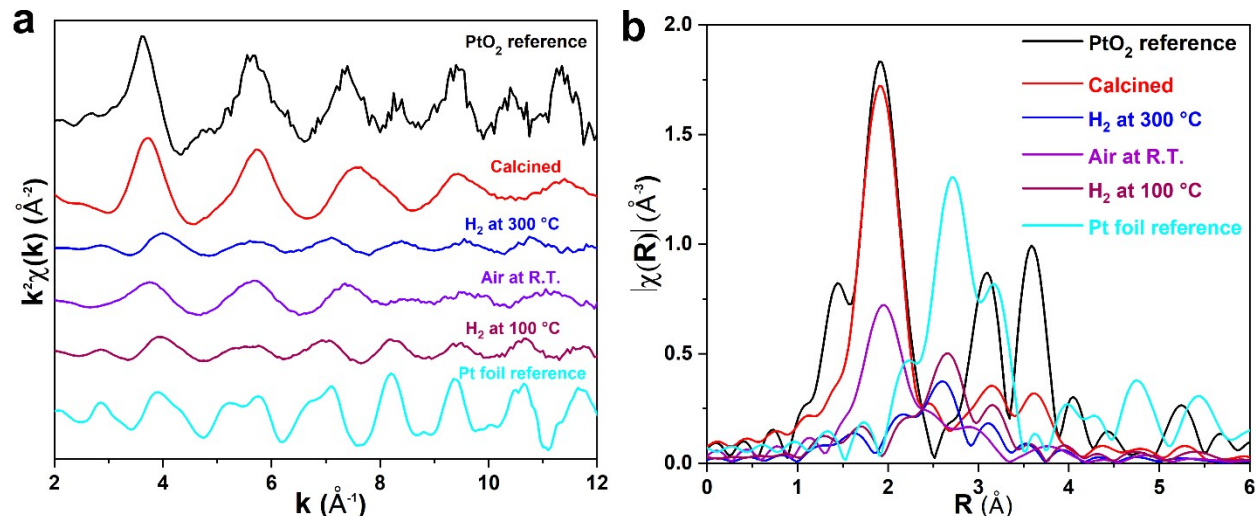


Fig. S8. (a) Pt L_3 -edge k^2 weighed EXAFS spectra and (b) Fourier transformed spectra of Pt@S-1-in-I prior to reduction, Pt@S-1-in-I under H₂ at 300 °C, after air exposure, and under H₂ at 100 °C.

EXAFS spectra were also measured to further support the XANES results. The Pt L_3 -edge EXAFS spectra and its corresponding Fourier transform (FT) of the catalyst are shown in Fig. S9. The EXAFS oscillations of calcined Pt@S-1-in-I prior to the reduction were found to be similar to that of the PtO₂ reference. A prominent peak was seen at 1.7 \AA in the Fourier transformed spectrum which is due to first shell Pt-O contribution.⁶ Two moderate peaks were observed centered on 3.2 and 3.6 \AA which are attributed to the contribution from Pt-Pt and Pt-O scattering paths of PtO₂. During the reduction at 300 °C, the oscillation attributed to PtO₂ scattering paths disappear and the oscillations resemble those of the Pt foil (Pt⁰) reference. The peak at 2.6 \AA in the Fourier transformed spectrum is attributed to the Pt-Pt first shell scattering path. The intensity of the EXAFS oscillations recorded after exposure to air at RT are lower than those of the calcined sample which is consistent with XANES outcomes and similarly indicate a partial oxidation of the catalyst. Finally, under H₂ at 100 °C the oscillations again closely resemble those of platinum foil. This provides a strong indication that reaction conditions in this work are sufficient to reduce the oxide shell that gets formed prior to the reaction.

Activity determination and encapsulation test

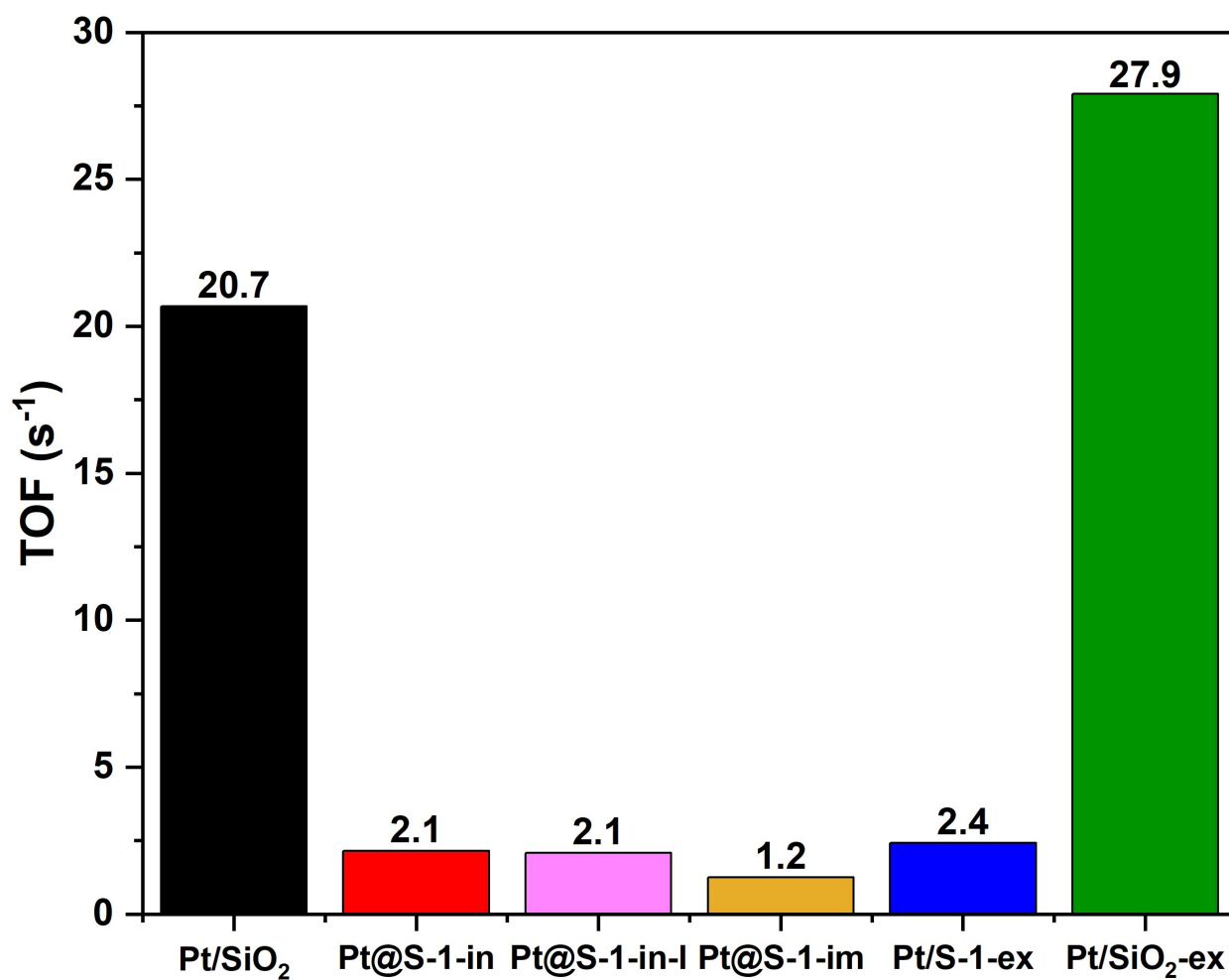


Fig. S9. Apparent TOFs in the hydrogenation of 1-hexene at room temperature determined at conversions below 70%. Reaction conditions: 1-hexene (4 mmol), 12 mg catalyst (5 mg for Pt/SiO₂), 100 μ l dodecane (internal standard), 60 ml abs. ethanol, 10 bar H₂, Room temperature, 800 RPM, 45 min (15 min for Pt/SiO₂, 9 min for Pt/SiO₂-ex).

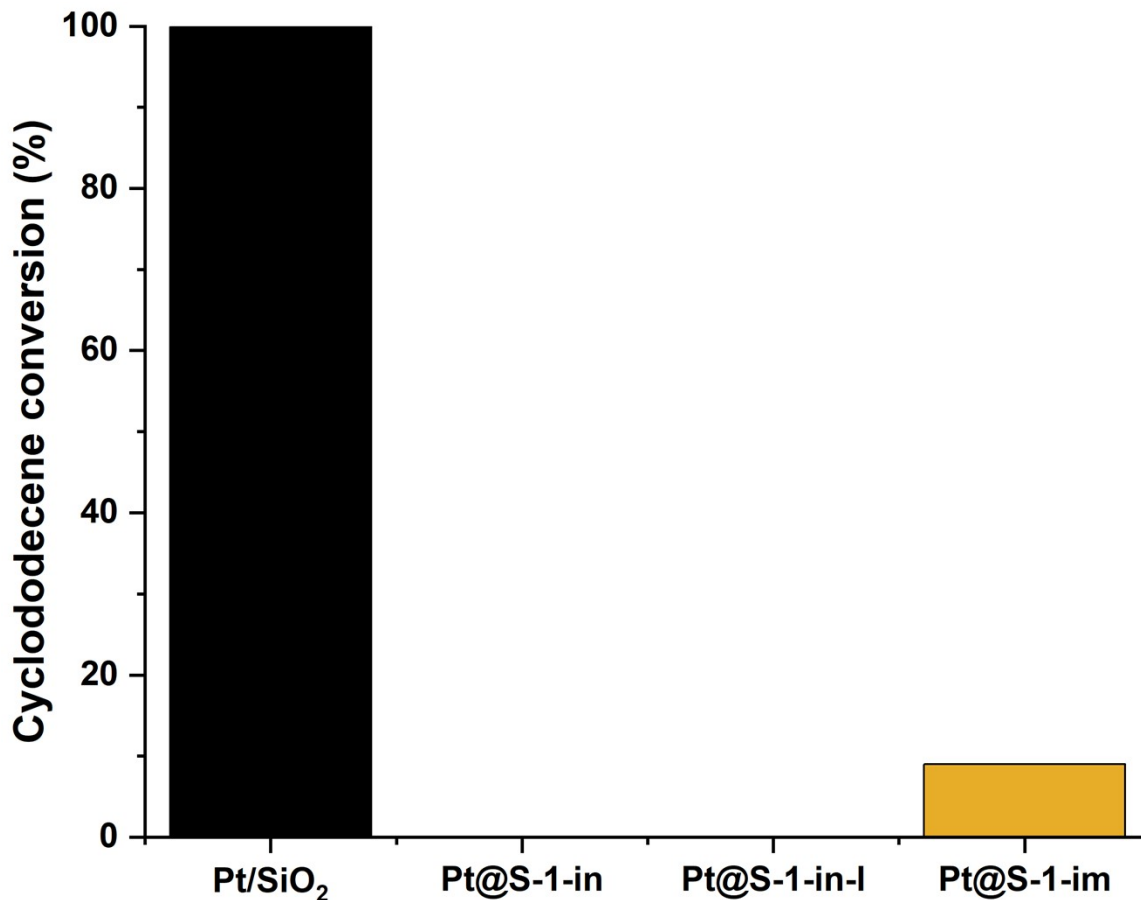


Fig. S10. Hydrogenation of cyclododecene over Pt-based catalysts after 24 h of heating at 80 °C. Reaction conditions: Catalyst (12.5 mg Pt/SiO₂, 25 mg Pt@S-1-in, 25 mg Pt@S-1-in-I or 27 mg Pt@S-1-im), Cyclododecene (0.5 mmol), dodecane (internal standard, 50 μl), ethanol (abs., 6 mL), P(H₂) = 10 bar T = 80 °C, t = 24 h.

The cyclododecene hydrogenation tests showed 9% conversion after 24 h for Pt@S-1-im. This low conversion indicates that most, but not all, metal is encapsulated. This is in agreement with STEM micrographs where a small number of large external platinum nanoparticles (>10 nm) were observed.

Cinnamaldehyde hydrogenation

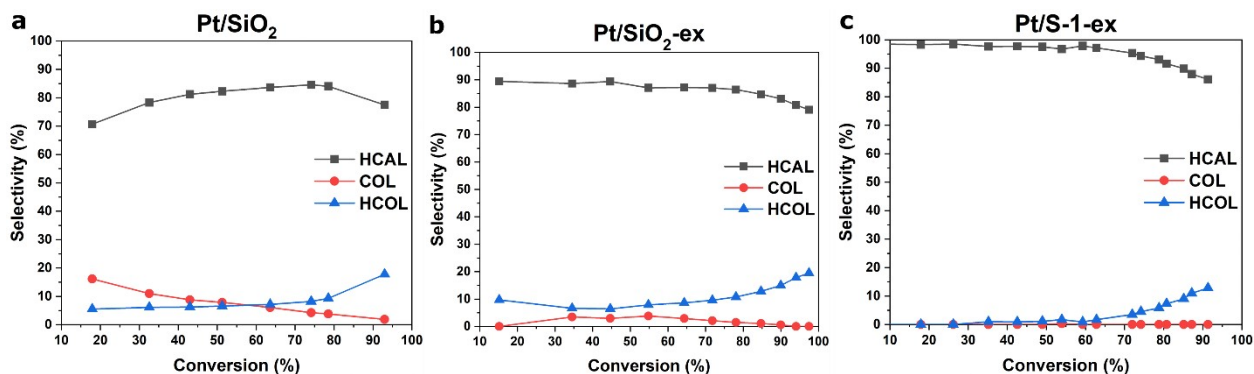


Fig. S11. Hydrocinnamaldehyde (HCAL), cinnamyl alcohol (COL), and hydrocinnamyl alcohol (HCOL) selectivity versus conversion of cinnamaldehyde (CAL) over surface supported catalysts (a) Pt/SiO₂, (b) Pt/SiO₂-ex, and (c) Pt/S-1-ex. Reaction conditions: 2.5

mmol CAL, Catalyst (144 mg Pt/SiO₂, 208 mg Pt/S-1-ex, 227 mg Pt/SiO₂-ex), 30 ml toluene, 250 μ l dodecane (internal standard), 10 bar H₂, 120 $^{\circ}$ C, 1000 rpm.

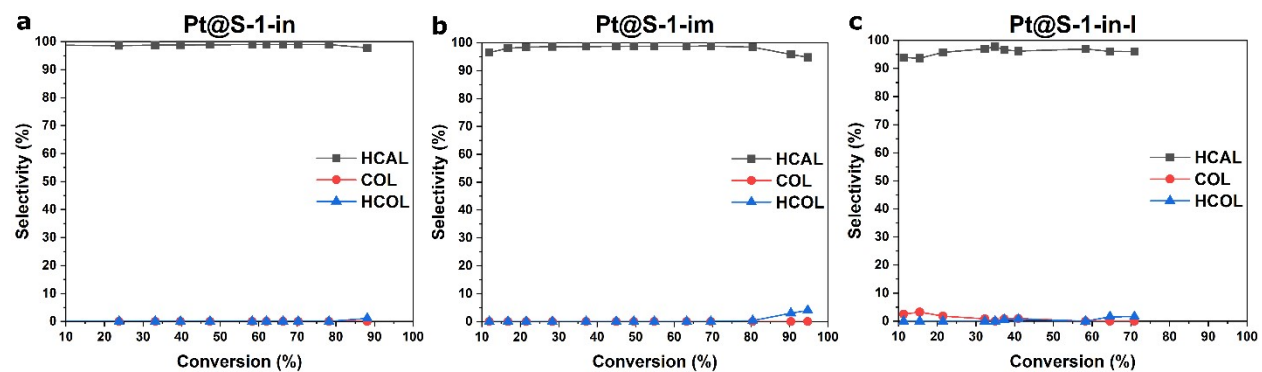


Fig. S12. Hydrocinnamaldehyde (HCAL), cinnamyl alcohol (COL), and hydrocinnamyl alcohol (HCOL) selectivity versus conversion of cinnamaldehyde (CAL) over the encapsulated catalysts (a) Pt@S-1-in, (b) Pt@S-1-im, and (c) Pt@S-1-in-I. Reaction conditions: 2.5 mmol CAL, Catalyst (293 mg Pt@S-1-in, 331 mg Pt@S-1-in-I, 294 mg Pt@S-1-im), 250 μ l dodecane (internal standard), 10 bar H₂, 120 $^{\circ}$ C, 1000 rpm.

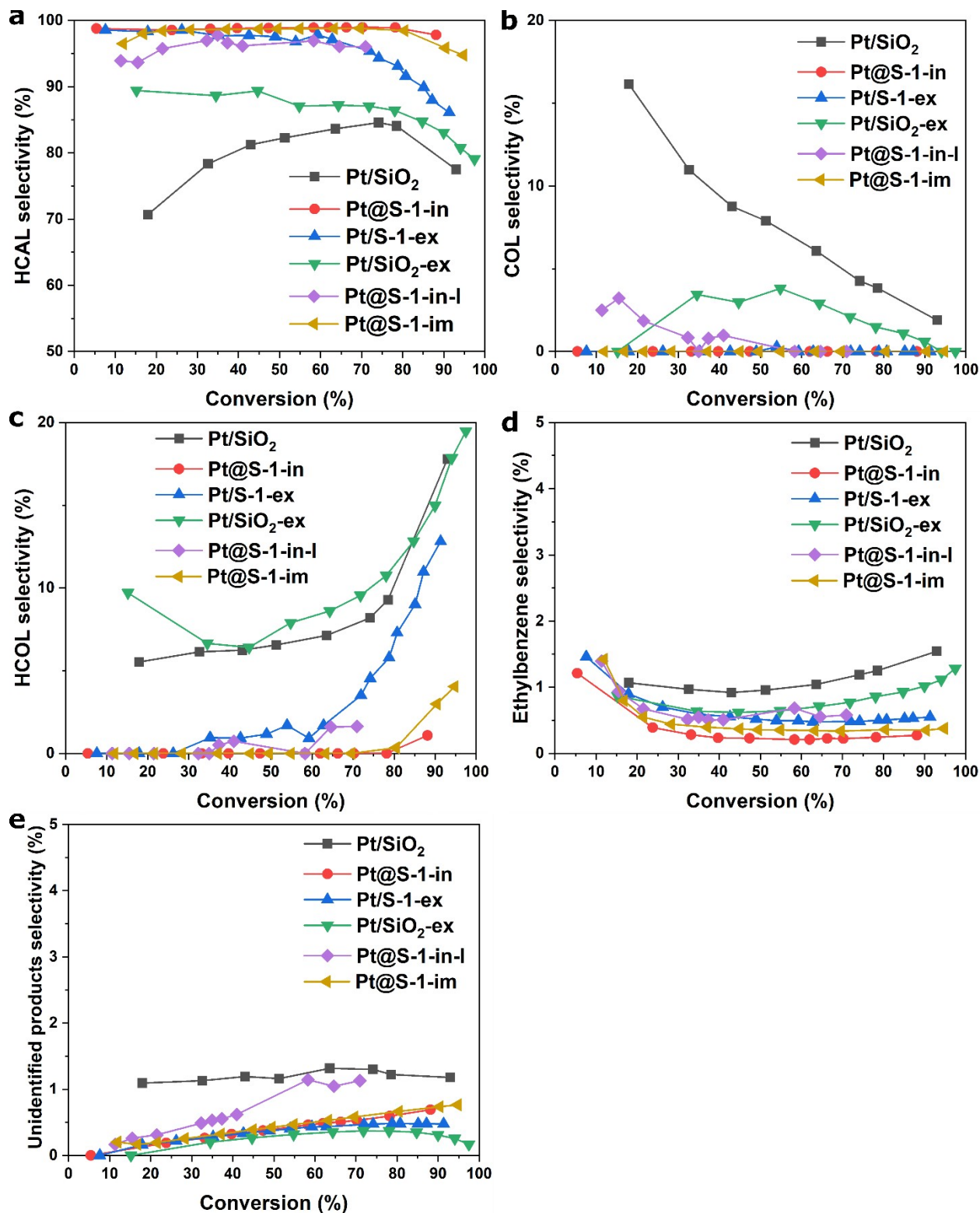


Fig. S13. Selectivity versus conversion of cinnamaldehyde (CAL) over the various catalysts to (a) hydrocinnamaldehyde (HCAL), (b) cinnamyl alcohol (COL), (c) hydrocinnamyl alcohol (HCOL), (d) ethylbenzene, (e) unidentified products. Reaction conditions: Catalyst (144 mg Pt/SiO₂, 293 mg Pt@S-1-in, 331 mg Pt@S-1-in-I, 294 mg Pt@S-1-im, 208 mg Pt/S-1-ex, 227 mg Pt/SiO₂-ex), 2.5 mmol CAL, 30 ml toluene, 250 μ l dodecane (internal standard), 10 bar H₂, 120 $^{\circ}$ C, 1000 rpm.

Support polarity

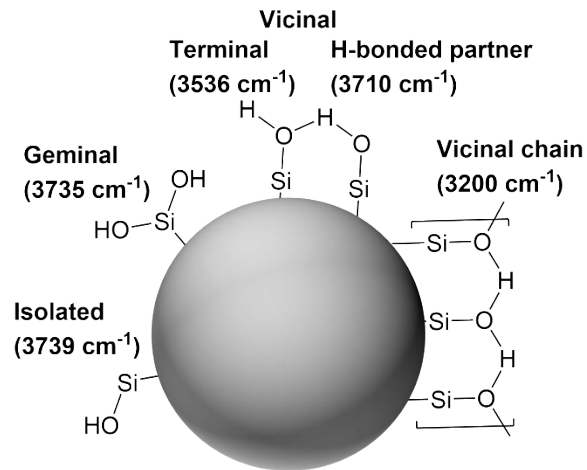


Fig. S14. The possible silanol groups in SiO₂-based materials and their FTIR band regions.⁷

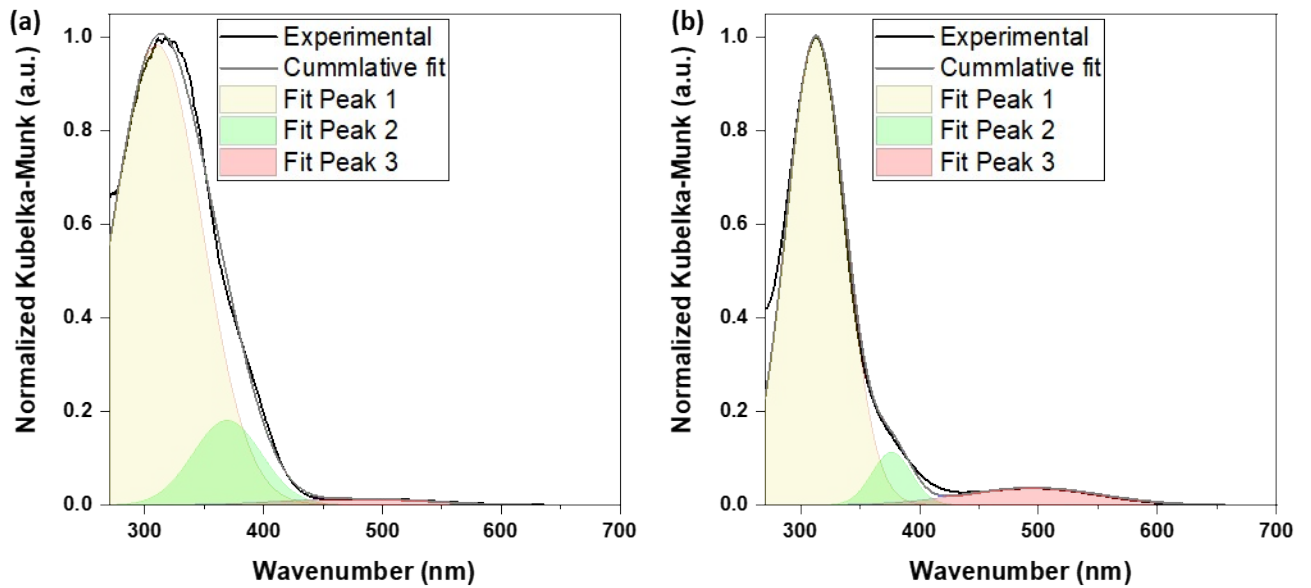


Fig. S15. Deconvolution of the normalized diffuse reflectance (DR) UV-vis spectra of (a) SiO₂ and (b) S-1 support obtained after adsorbing Reichard's dye.

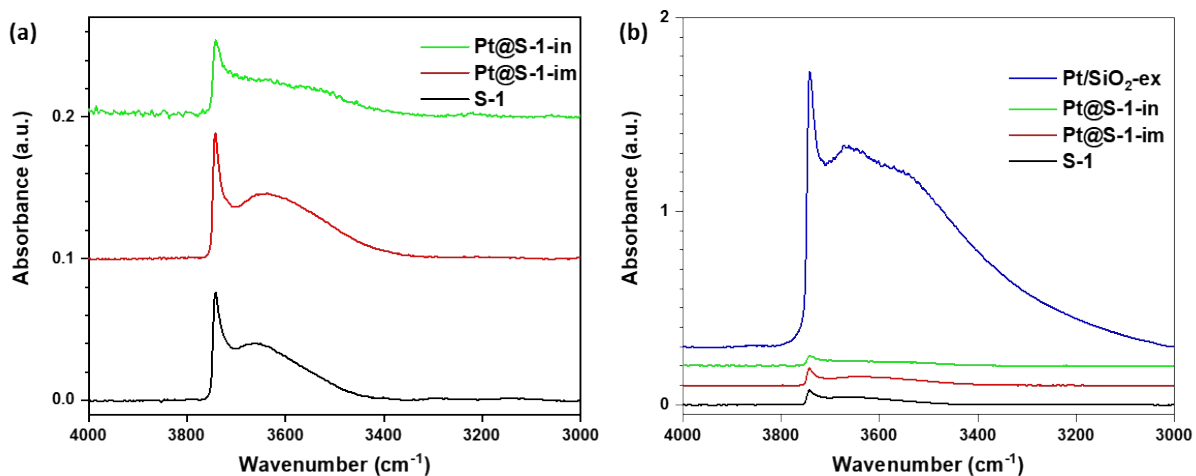


Fig. S16. FTIR spectra showing the silanol bands of the samples (a) Pt@S-1-in, Pt@S-1-im, and S-1, (b) the same samples compared to Pt/SiO₂-ex.

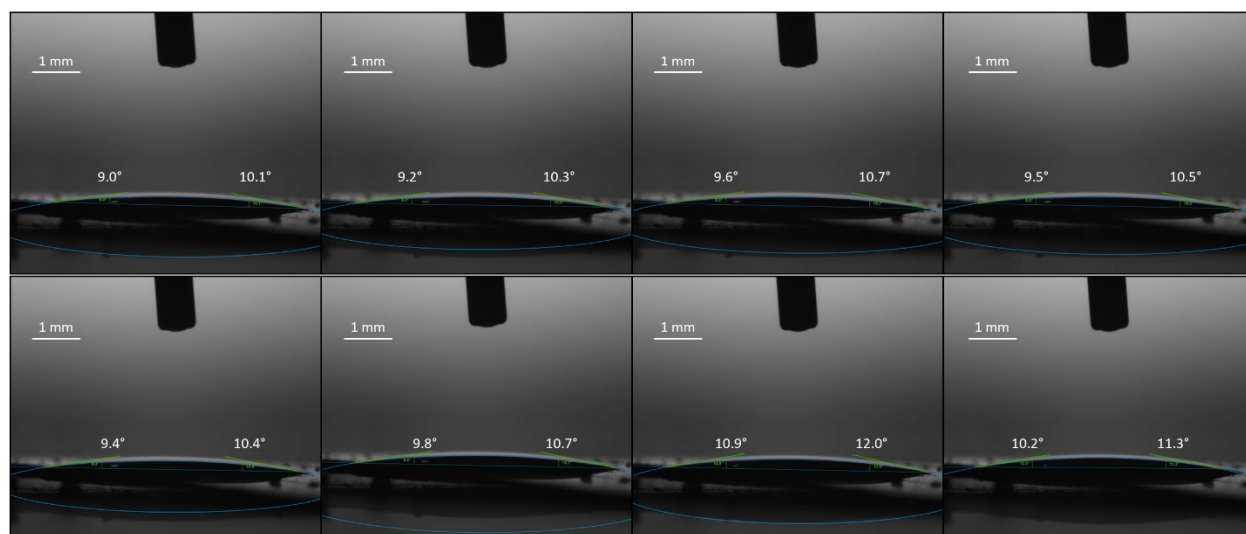


Fig. S17. Measurement of the dH₂O contact angle with the SiO₂ support.

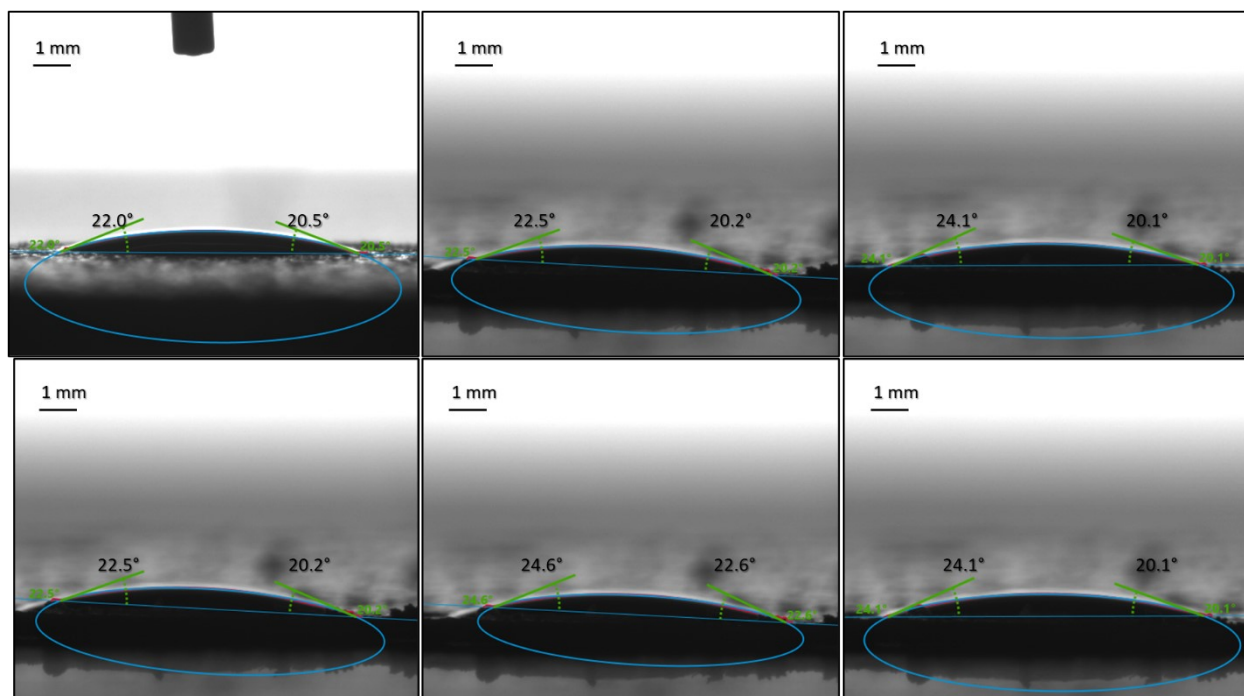


Fig. S18. Measurement of the dH₂O contact angle with the Silicalite-1, support.

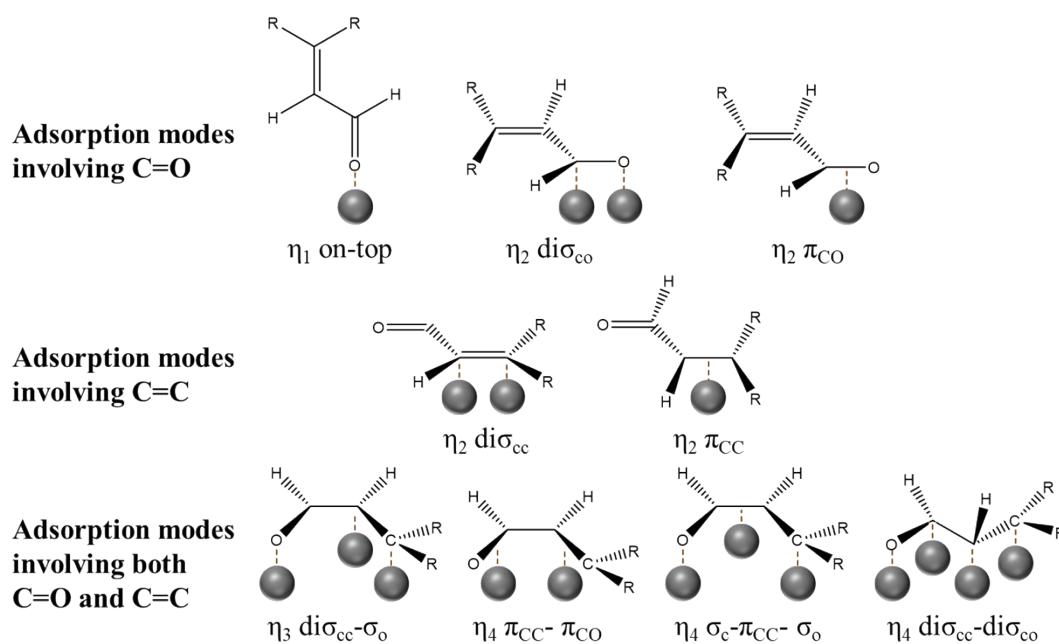


Fig. S19. The possible adsorption configurations of conjugated unsaturated aldehydes on metal NPs. Based on ref. ⁸

Shell representation

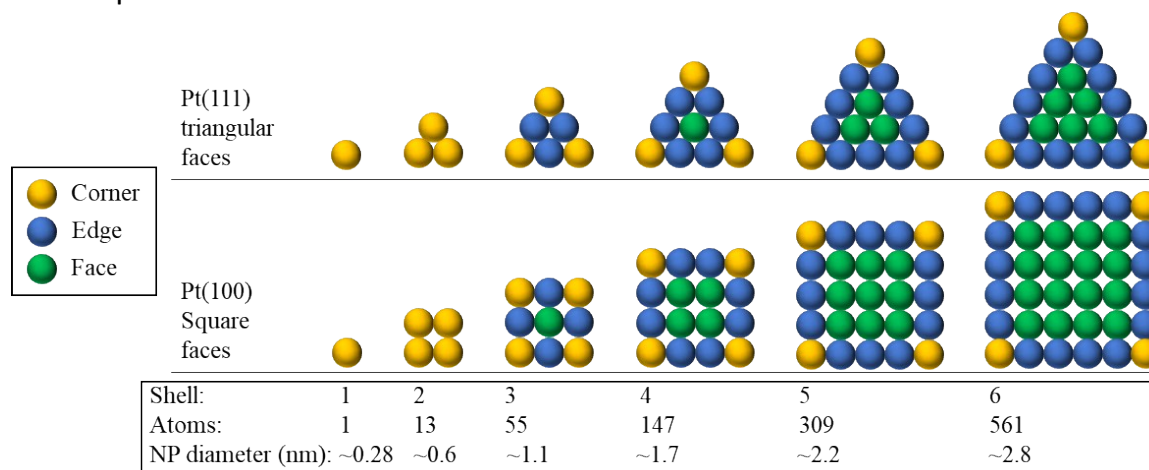


Fig. S20. A visual representation of the corner, edge, and face sites of perfect cuboctahedral particles vs the NP diameter and shell number.⁹ Pt(111) has a triangular faces and Pt(100) has square faces.

CO chemisorption

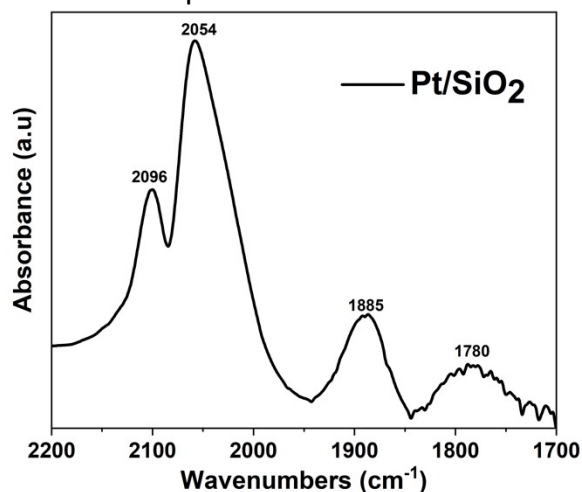


Fig. S21. CO chemisorbed on Pt/SiO₂ showing CO linearly adsorbed on Pt (2096 cm⁻¹, 2054 cm⁻¹) and CO adsorbed in a bridged configuration between two Pt atoms. (1885 cm⁻¹ and 1780 cm⁻¹).

The band around 2096 cm⁻¹ in Pt/SiO₂ was previously attributed to CO linearly adsorbed on large Pt⁰ NPs.¹⁰ Particularly, it corresponds to adsorption on extended Pt surfaces like Pt(111) and Pt(100) face sites present on the surface.¹¹ The band centered at 2054 cm⁻¹ correspond to a combination of mostly linearly adsorbed CO on low coordination Pt⁰ surface sites¹¹⁻¹³ and Pt(111) CO bonded sites¹⁴ Finally, the bands at 1885 and 1780 cm⁻¹ are associated with CO adsorbed in a bridged configuration between two Pt atoms.¹²

Recyclability test

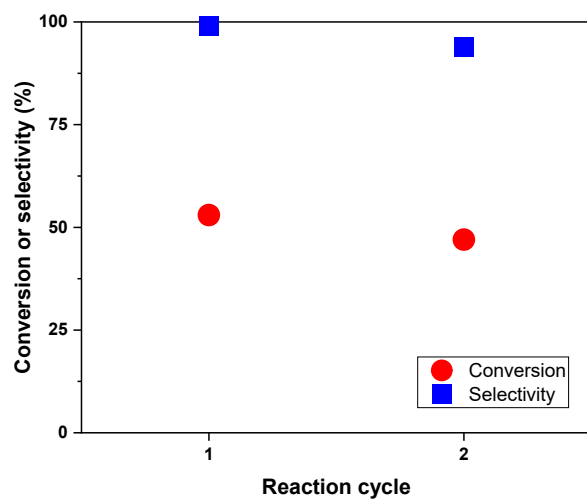


Fig. S22. Recycling experiment with Pt@S-1-in in the CAL hydrogenation. New CAL is added to compensate the consumed reactant prior to the second cycle.

Supplementary tables

Table S1. Textural properties of the calcined catalysts determined from nitrogen physisorption.

Catalyst	SBET (m ² .g ⁻¹)	V mic (cm ³ .g ⁻¹)
Pt@S-1-in	381	0.13
Pt@S-1-in-l	403	0.14
S-1	374	0.11
Pt@S-1-im	394	0.11
Pt/S-1-ex	368	0.13
Pt/SiO ₂ -ex	305	-
Pt/SiO ₂	326	-

Table S2. ICP-OES Elemental analysis of the various catalysts.

Catalyst	Pt loading by ICP
Pt@S-1-in	0.40 wt%
Pt@S-1-in-l	0.26 wt%
Pt@S-1-im	0.37 wt%
Pt/S-1-ex	0.49 wt%
Pt/SiO ₂ -ex	0.45 wt%

Table S3. 1-hexene hydrogenation over Pt-based catalysts.

Catalyst	n _{conv} /(n _{pt} · h)	Dispersion ^c	Apparent TOF
Pt/SiO ₂ ^a	32161	0.43	74446
Pt@S-1-in	6652	0.86	7735
Pt@S-1-in-l	6832	0.91	7508
Pt@S-1-im	2949	0.66	4495
Pt/S-1-ex	4652	0.53	8746
Pt/SiO ₂ -ex ^b	59189	0.59	100491

Reaction conditions: 1-hexene (4 mmol), 12 mg catalyst, 100 μl dodecane (internal standard), 60 ml abs. ethanol, 10 bar H₂, Room temperature, 800 RPM, 45 min. (a) 5 mg catalyst, 15 min reaction time. (b) 9 min reaction time. (c) Determined using the average particle size determined through STEM by assuming perfect cuboctahedral particles.

Table S4. Water contact angles (CA) on the SiO₂ and S-S-1 supports.

Pt/SiO ₂			S-1		
CA(L) [°]	CA(R) [°]	CA(av) [°]	CA(L) [°]	CA(R) [°]	CA(av) [°]
9	10.1	9.6	22	20.5	21.3
9.2	10.3	9.8	23.2	20.4	21.8
9.6	10.7	10.2	22.5	20.2	21.4
9.5	10.5	10.0	24.1	20.1	22.1
9.4	10.4	9.9	22.5	20.2	21.4
9.8	10.7	10.3	24.6	22.6	23.6
10.9	12	11.5	24.1	20.1	22.1
10.2	11.3	10.8			
10	10.6	10.3			

$\Theta_{av} = 10.2^\circ$	$\Theta_{av} = 21.9^\circ$
----------------------------	----------------------------

Encapsulation test

Table S5. Cyclododecene conversion over Pt-based catalysts.

Catalyst	Cyclododecene conversion (%)
Pt/SiO ₂	100
Pt@S-1-in	0
Pt@S-1-in-l	0
Pt@S-1-im	9

Catalyst: 12.5 mg Pt/SiO₂, 25 mg Pt@S-1-in, 25 mg Pt@S-1-in-l, 27 mg Pt@S-1-im, Cyclododecene (0.5 mmol), dodecane (internal standard, 50 μ l), ethanol (abs., 6 mL), P(H₂) = 10 bar T = 80 °C, t = 24 h.

Cinnamaldehyde hydrogenation

Table S6. Cinnamaldehyde conversion and product distribution over Pt/SiO₂.

Time (h)	Conversion (%)	HCAL selectivity (%)	COL selectivity (%)	HCOL selectivity (%)	Ethylbenzene selectivity (%)	Unknowns (%)
1	17.9	70.7	16.2	5.5	1.1	1.1
2	32.6	78.3	11.0	6.1	1.0	1.1
3	43.0	81.2	8.8	6.2	0.9	1.2
4	51.3	82.3	7.9	6.6	1.0	1.2
5	63.6	83.6	6.1	7.1	1.0	1.3
7	74.1	84.6	4.3	8.2	1.2	1.3
8	78.5	84.1	3.8	9.3	1.3	1.2
24	93.0	77.5	1.9	17.8	1.5	1.2

Reaction conditions: 2.5 mmol CAL, 144 mg Pt/SiO₂, 30 ml toluene, 250 μ l dodecane (internal standard), 10 bar H₂, 120 °C, 1000 rpm.

Table S7. Cinnamaldehyde conversion and product distribution over Pt@S-1-in.

Time (h)	Conversion (%)	HCAL selectivity (%)	COL selectivity (%)	HCOL selectivity (%)	Ethylbenzene selectivity (%)	Unknowns (%)
1	5.4	98.8	0.0	0.0	1.2	0.0
2	23.8	98.6	0.0	0.0	0.4	0.2
3	33.2	98.7	0.0	0.0	0.3	0.3
4	39.7	98.8	0.0	0.0	0.2	0.3
5	47.4	98.9	0.0	0.0	0.2	0.4
7	58.3	98.9	0.0	0.0	0.2	0.5
8	62.0	98.9	0.0	0.0	0.2	0.5
10	66.3	98.9	0.0	0.0	0.2	0.5
12	70.2	99.0	0.0	0.0	0.2	0.5
24	78.2	98.9	0.0	0.0	0.2	0.6
48	88.1	97.8	0.0	1.1	0.3	0.7

Reaction conditions: 2.5 mmol CAL, 293 mg Pt@S-1-in, 30 ml toluene, 250 μ l dodecane (internal standard), 10 bar H₂, 120 °C, 1000 rpm.

Table S8. Cinnamaldehyde conversion and product distribution over Pt@S-1-in-l.

Time (h)	Conversion (%)	HCAL selectivity (%)	COL selectivity (%)	HCOL selectivity (%)	Ethylbenzene selectivity (%)	Unknowns (%)
2	11.3	93.9	2.5	0.0	1.4	0.2
3	15.5	93.7	3.2	0.0	0.9	0.3
4	21.5	95.7	1.9	0.0	0.7	0.3
5	32.3	97.0	0.8	0.0	0.5	0.5
6	35.0	97.8	0.0	0.0	0.5	0.5
7	37.3	96.6	0.8	0.5	0.5	0.6
8	41.0	96.2	1.0	0.7	0.5	0.6
25	58.3	96.9	0.0	0.0	0.7	1.1
30	64.6	96.1	0.0	1.6	0.6	1.0
48	70.9	96.0	0.0	1.6	0.6	1.1

Reaction conditions: 2.5 mmol CAL, 331 mg Pt@S-1-in-l, 30 ml toluene, 250 μ l dodecane (internal standard), 10 bar H₂, 120 °C, 1000 rpm.

Table S9. Cinnamaldehyde conversion and product distribution over Pt@S-1-im.

Time (h)	Conversion (%)	HCAL selectivity (%)	COL selectivity (%)	HCOL selectivity (%)	Ethylbenzene selectivity (%)	Unknowns (%)
1	11.9	96.5	0.0	0.0	1.4	0.2
2	16.8	98.0	0.0	0.0	0.8	0.2
3	21.5	98.4	0.0	0.0	0.6	0.2
4	28.3	98.6	0.0	0.0	0.4	0.3
5	37.1	98.7	0.0	0.0	0.4	0.3
6	44.9	98.7	0.0	0.0	0.4	0.4
7	49.5	98.7	0.0	0.0	0.4	0.4
8	54.9	98.8	0.0	0.0	0.4	0.5
10	63.3	98.8	0.0	0.0	0.3	0.5
12	69.6	98.8	0.0	0.0	0.3	0.6
24	80.5	98.5	0.0	0.3	0.4	0.7
48	90.4	95.8	0.0	3.0	0.4	0.7
71.5	94.8	94.8	0.0	4.0	0.4	0.8

Reaction conditions: 2.5 mmol CAL, 294 mg Pt@S-1-im, 30 ml toluene, 250 μ l dodecane (internal standard), 10 bar H₂, 120 °C, 1000 rpm.

Table S10. Cinnamaldehyde conversion and product distribution over Pt/S-1-ex.

Time (h)	Conversion (%)	HCAL selectivity (%)	COL selectivity (%)	HCOL selectivity (%)	Ethylbenzene selectivity (%)	Unknowns (%)
2	7.6	98.5	0.0	0.0	1.5	0.0
3	17.9	98.3	0.0	0.0	0.9	0.2
4	26.2	98.5	0.0	0.0	0.7	0.2
5	35.2	97.7	0.0	1.0	0.6	0.3
6	42.6	97.7	0.0	0.9	0.6	0.3

7	49.0	97.6	0.0	1.2	0.5	0.4
8	53.9	96.8	0.3	1.7	0.5	0.4
10	59.3	97.9	0.0	0.9	0.5	0.4
12	62.8	97.1	0.0	1.7	0.5	0.4
24	71.9	95.3	0.0	3.5	0.5	0.5
32	74.2	94.3	0.0	4.5	0.5	0.5
48	78.8	93.1	0.0	5.8	0.5	0.5
56	80.7	91.6	0.0	7.3	0.5	0.5
72	85.1	89.9	0.0	9.0	0.5	0.5
80	87.2	87.9	0.0	11.0	0.5	0.5
97.66	91.3	86.1	0.0	12.8	0.6	0.5

Reaction conditions: 2.5 mmol CAL, 208 mg Pt/S-1-ex, 30 ml toluene, 250 μ l dodecane (internal standard), 10 bar H₂, 120 °C, 1000 rpm.

Table S11. Cinnamaldehyde conversion and product distribution over Pt/SiO₂-ex.

Time (h)	Conversion (%)	HCAL selectivity (%)	COL selectivity (%)	HCOL selectivity (%)	Ethylbenzene selectivity (%)	Unknowns (%)
1	15.2	89.4	0.0	9.7	0.9	0.0
2	34.5	88.6	3.4	6.7	0.6	0.2
3	44.7	89.4	3.0	6.4	0.6	0.3
4	54.8	87.1	3.8	7.9	0.6	0.3
5	64.3	87.2	2.9	8.6	0.7	0.4
6	71.8	87.0	2.1	9.6	0.8	0.4
7	78.1	86.4	1.5	10.8	0.9	0.4
8	84.7	84.7	1.1	12.8	0.9	0.4
9	90.0	83.1	0.6	15.0	1.0	0.3
10	94.1	80.8	0.0	17.9	1.1	0.3
11	97.5	79.1	0.0	19.5	1.3	0.2
12	99.2	70.4	0.0	28.2	1.4	0.0

Reaction conditions: 2.5 mmol CAL, 227 mg Pt/SiO₂-ex, 30 ml toluene, 250 μ l dodecane (internal standard), 10 bar H₂, 120 °C, 1000 rpm.

Table S12. Cinnamaldehyde conversion over Silicalite-1 (blank test).

Time (h)	Conversion (%) ^a
49	1.9

^aNo products were identified. Reaction conditions: 2.5 mmol CAL, 300 mg S-1, 30 ml toluene, 250 μ l dodecane (internal standard), 10 bar H₂, 120 °C, 1000 rpm.

The products in the blank reaction were near the detection limits of the instrument and no reliable selectivity could be determined.

Table S13. Cinnamaldehyde conversion and product distribution over Pt@S-1-in-I under literature conditions.¹⁵

Time (h)	Conversion (%)	HCAL selectivity (%)	COL selectivity (%)	HCOL selectivity (%)	Ethylbenzene selectivity (%)	Unknowns (%)
1	8.3	52.4	47.6	0.0	0	0.3
2	17.9	31.8	68.2	0.0	0	0.5

3	23.5	29.1	69.5	1.4	0	0.9
4	28.9	30.1	68.7	1.2	0	1.1
5	32.3	27.6	71.3	1.1	0	1.3
6	33.6	29.8	68.6	1.5	0	1.6
7	34.1	30.0	67.8	2.3	0	2.0
8	34.9	31.8	65.9	2.3	0	2.1
10	34.5	29.5	67.9	2.6	0	2.2
11.5	36.8	30.6	66.6	2.8	0	2.2
24.5	64.7	49.0	47.4	3.7	0	2.7
48	86.7	60.6	34.4	5.1	0	2.4

Reaction conditions: 2.5 mmol CAL, 258 mg Pt@S-1-in-I (1:763 Pt:CAL), 30 ml methanol, 250 μ l dodecane (internal standard), 10 bar H₂, 60 °C, 800 rpm.¹⁵

Table S14 Comparison of the initial TOF and the initial rate of C=O hydrogenation for the cinnamaldehyde hydrogenations over Pt@S-1-in-I in toluene and methanol.

Solvent	Catalyst dispersion	Apparent TOF (h ⁻¹)	CAL:Pt	Initial rate of CAL C=O consumption (mol·l ⁻¹ ·h ⁻¹)
Toluene	0.91	48	567	0.02 · 10 ⁻²
Methanol ^a	0.91	72	727	0.51 · 10 ⁻²

Reaction conditions: 2.5 mmol CAL, 331 mg Pt@S-1-in-I, 30 ml toluene, 250 μ l dodecane (internal standard), 10 bar H₂, 120 °C, 1000 rpm. ^aReaction performed with 258 mg Pt@S-1-in-I in 30 ml methanol at 60 °C.

The Initial rate of CAL C=O consumption was determined by multiplying the initial rate with the selectivity to products where the C=O is hydrogenated (COL, HCOL).

References

- O. Proux, X. Biquard, E. Lahera, J. J. Menthonnex, A. Prat, O. Ulrich, Y. Soldo, P. Trévisson, G. Kapoujyan, G. Perroux, P. Taunier, D. Grand, P. Jeantet, M. Deleglise, J. P. Roux and J. L. Hazemann, *Physica Scripta T*, 2005, **T115**, 970–973.
- A. Aguilar-Tapia, S. Ould-Chikh, E. Lahera, A. Prat, W. Delnet, O. Proux, I. Kieffer, J. M. Basset, K. Takanabe and J. L. Hazemann, *Review of Scientific Instruments*, 2018, **89**, 035109.
- B. Ravel and M. Newville, in *Journal of Synchrotron Radiation*, International Union of Crystallography, 2005, vol. 12, pp. 537–541.
- L. S. R. Kumara, O. Sakata, H. Kobayashi, C. Song, S. Kohara, T. Ina, T. Yoshimoto, S. Yoshioka, S. Matsumura and H. Kitagawa, *Sci Rep*, 2017, **7**, 1–11.
- D. C. Koningsberger, M. K. Oudenhuijzen, J. H. Bitter and D. E. Ramaker, *Top Catal*, 2000, **10**, 167–177.
- C. Dessal, T. Len, F. Morfin, J. L. Rousset, M. Aouine, P. Afanasiev and L. Piccolo, *ACS Catal*, 2019, **9**, 5752–5759.
- L. J. Durndell, C. M. A. Parlett, N. S. Hondow, M. A. Isaacs, K. Wilson and A. F. Lee, *Sci Rep*, 2015, **5**, 1–9.

- 8 M. Deng, D. Wang and Y. Li, *Appl Catal A Gen*, 2023, 666, 119423.
- 9 J. Aarons, M. Sarwar, D. Thompsett and C.-K. Skylaris, *J Chem Phys*, 2016, **145**, 220901.
- 10 R. K. Brandt, M. R. Hughes, L. P. Bourget, K. Truskowska and R. G. Greenler, *Surf Sci*, 1993, **286**, 15–25.
- 11 A. Corma, P. Serna, P. Concepción and J. J. Calvino, *J Am Chem Soc*, 2008, **130**, 8748–8753.
- 12 P. Bazin, O. Saur, J. C. Lavalley, M. Daturi and G. Blanchard, *Physical Chemistry Chemical Physics*, 2005, **7**, 187–194.
- 13 V. Perrichon, L. Retailleau, P. Bazin, M. Daturi and J. C. Lavalley, *Appl Catal A Gen*, 2004, **260**, 1–8.
- 14 C. Lentz, S. P. Jand, J. Melke, C. Roth and P. Kaghazchi, *J Mol Catal A Chem*, 2017, **426**, 1–9.
- 15 C. Liu, P. Zhu, J. Wang, H. Liu and X. Zhang, *Chemical Engineering Journal*, 2022, **446**, 137064.